

DALTON TRANSACTIONS (ISSN: 1477-9226) (eISSN: 1477-9234) 44(37):
16352-16360. (2015)

DOI: 10.1039/C5DT02750K



Stereoselective coordination: a six-membered P,N-chelate tailored for asymmetric allylic alkylation

Received 00th January 20xx,
Accepted 00th January 20xx

DOI: 10.1039/x0xx00000x

www.rsc.org/

Six-membered chelate complexes $[\text{Pd}(\mathbf{1a-b})\text{Cl}_2]$, $(\mathbf{2a-b})$ and $[\text{Pd}(\mathbf{1a-b})(\eta^3\text{-PhCHCHCHPh})]\text{BF}_4$, $(\mathbf{3a-b})$ of P,N-type ligands **1a**, ((2S, 4S)-2-diphenyl-phosphino-4-isopropylamino-pentane) and **1b**, ((2S, 4S)-2-diphenyl-phosphino-4-methylamino-pentane) have been prepared. The Pd-complexes have been characterized in solution by 1D and 2D NMR spectroscopy. The observed structures were confirmed by DFT calculations and in case of **2a** also by X-ray crystallography. Unexpectedly, the coordination of the all-carbon-backbone aminophosphine **1a** resulted in not only a stereospecific locking of the donor nitrogen atom into one of the two possible configurations but also the conformation of the six-membered chelate rings containing three alkyl substituents was forced into the same single chair structure showing axially placed isopropyl group on the coordinated N-atom. The stereodiscriminative complexation of **1a** led to the formation of a palladium catalyst with a conformationally rigid chelate having a configurationally fixed nitrogen and electronically different coordination sites due to the presence of P and N donors. The stereochemically fixed catalyst provided excellent ee's (up to 96%) and activities in asymmetric allylic alkylation reactions. In contrast, the chelate rings formed by **1b** exist in two different chair conformations, both containing axial methyl groups, but with the opposite configurations of the coordinated N-atom. Pd-complexes of **1b** provided low enantioselectivities in similar alkylations, therefore emphasizing the importance of the stereoselective coordination of N-atom in analogous P-N chelates. The factors determining the coordination of the ligands were also studied with respect to the chelate ring conformation and the nitrogen configuration.

Introduction

In asymmetric synthesis, the application of transition metal catalysts containing chiral donor atoms is a fruitful approach for achieving high enantioselectivities.¹ The potential of these systems is due to the ability of an efficient transfer of chirality from the catalyst to the substrate. A challenging direction of research in asymmetric synthesis is the design of new catalysts that are composed of metal-ligand assemblies with meta-stable stereochemistries, i.e. the ligand structure is held in a specific spatial arrangement solely due to metal coordination.² In this respect, ligands with chiral backbone and with stereogenic N-donors are of great interest. However, it is important to note that the selectivity of the nitrogen coordination depends on a number of factors such as the effect of the *cis* halogen ligand in the square planar dihalogene complexes, the coordination properties of the solvent, the entropy connected with the fluxionality of the possible conformers or even the coordination sphere of the metal.³

The formation and control of a stereogenic nitrogen center that is directly attached to the metal increases the likelihood of effective stereochemical communication between the ligand and the reactive site. Furthermore, with heterobidentate aminoalkyl-phosphine (P,N)

ligands the difference in *trans* influence between the P and N donor atoms differentiates the two binding sites electronically, making the ligand *trans* to the phosphorus more labile. The features listed above are important in asymmetric catalysis⁴, which can be sensitive for very fine stereochemical changes in the ligand nature.

The coordination chemistry and catalytic properties of P,N-ligands with chiral all-carbon backbone and chiral nitrogen donor has been previously investigated for 5-membered chelates.⁵ However, the coordination behaviour of six-membered chelating P,N-ligands with stereogenic nitrogen has scarcely been studied and is far more complicated because of the configurational isomerism of nitrogen and the possible conformational changes associated with a C₁-symmetry six-membered ring.

Previously, Chan and Spilling reported on the catalytic application of N-chiral six-membered chelating phosphinite-amine (POC_nN) and aminophosphine-amine (PNC_nN) ligands.⁶ In an extensive study, Petit *et al.* described the synthesis of chiral PNC_nN type ligands and investigated the importance of N-chirality in asymmetric catalysis.⁷ However, no clear interpretation of the factors influencing the stereoselective coordination via both the ring conformation and the nitrogen configuration has been available yet for such systems. Undoubtedly, through understanding of these factors, the coordination behaviour of the ligands could be regulated as a crucial part of structure tailoring in catalysis⁸ and even in medicinal chemistry.⁹

Recently, we have synthesized a new class of chiral pentane-2,4-diyl-based ligands, capable of forming six-membered chelate rings.¹⁰ Using these ligands we envisaged to unite (i) the relative conformational rigidity provided by the pentane-2,4-diyl backbone with (ii) the stereoselective coordination of the nitrogen, (iii) the electronic differentiation induced by the difference of donor groups and (iv) the modular ligand structure associated with a convenient

^a Department of Organic Chemistry, University of Pannonia, Egyetem u. 10, H-8200 Veszprém, Hungary.

^b Department of Physical Chemistry, University of Debrecen, Egyetem tér 1, H-4032 Debrecen, Hungary.

^c Institute of Materials and Environmental Chemistry, Hungarian Academy of Sciences, P.O. Box 17, H-1525 Budapest, Hungary.

† Electronic Supplementary Information (ESI) available: NMR spectra of complexes **2a-b** and **3a-b**, details of DFT calculations, X-ray crystallographic data. See DOI: 10.1039/x0xx00000x

synthesis. We have found that Pd-complexes of ligand **1a** (Figure 1) give high activities and enantioselectivities in asymmetric allylic alkylation reactions. Motivated by this observation, we have combined multinuclear 1D and 2D NMR spectroscopy, X-ray crystallography and electronic structure theory (DFT) calculations to characterize and understand the coordination and structural chemistry of the six-membered palladium chelates of ligands **1a** and **1b**, containing sterically larger N-isopropyl (N-iPr) and smaller N-methyl (N-Me) substituents, respectively (Figure 1.). The importance of the stereoselective coordination of such N-atoms in asymmetric allylic alkylation is highlighted.

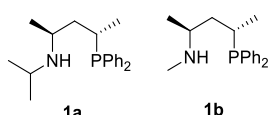
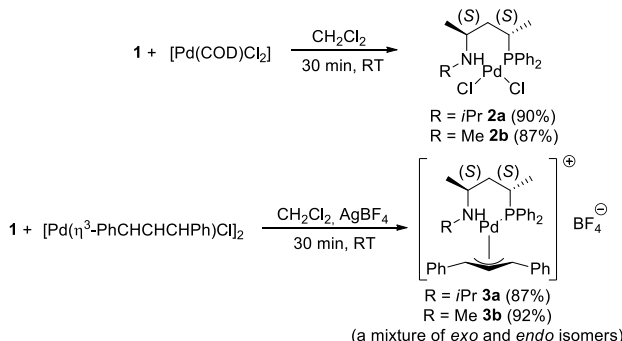


Figure 1. Pentane-2,4-diyliidene based aminoalkyl phosphines

Results and discussion

Synthesis of Pd-complexes and their structural characterization

Synthesis. Complexes **2a-b** and **3a-b** were prepared from suitably labile precursors to promote chelate formation according to Scheme 1. Considering the two possible nitrogen configurations and the conformations of the chelate, four chair, 12 twist-boat and 12 boat isomers can be drawn for complexes **2** (Figure 2).¹¹ The widely used puckering parameters to describe the ring conformation have limited applicability in our case because of the large difference in the C-C covalent and M-P or M-N coordination bond distances.¹²



Scheme 1. Synthesis of complexes **2a-b** and **3a-b**

NMR analysis of complexes 2. Complex **2a** was investigated by ¹H, ¹³C{¹H}, ³¹P{¹H}, ¹H-¹H-COSY, ¹H-¹H NOESY and HMQC NMR methods using CDCl₃ or CD₂Cl₂ as solvents. According to the NMR data only one diastereomer can be found in solution. Cooling the sample in CD₂Cl₂ to -80 °C the ³¹P{¹H} NMR spectrum still shows only a single line.

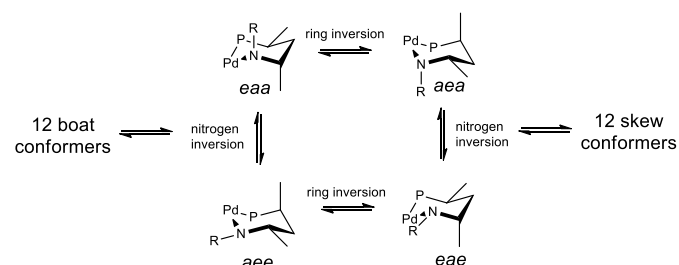


Figure 2. Stereoisomers of **2** ($R = i\text{Pr}$ or Me , Cl ligands are omitted for clarity)

In the ¹H NMR spectrum the observed large ~34.5 Hz couplings of ³J(P,H^d) (close to the Karplus maximum)¹³ and the large geminal ²J(H^c,H^d) couplings (-15.6 Hz)¹⁴ are only possible in a chair conformation (Figure 3). The relatively small ³J(P,H^b) couplings (~12 Hz) indicates an equatorial position of the Me groups next to P.¹³ The values of ³J(H^e,H^c) = 3.2 Hz, ³J(H^e,H^d) = 2.9 Hz and ³J(H^a,H^d) = 3.6 Hz suggest torsion angles of approximately 60° between the corresponding hydrogen atoms, while based on the coupling ³J(H^a,H^c) = 13.5 Hz a ca. 180° torsion angle can be assumed. Since only the ³J(H^{ax},H^{ax}) is expected to be large and both ³J(H^{ax},H^{eq}) and ³J(H^{eq},H^{eq}) to be small, we can conclude that the methyl groups CH₃^b and CH₃^f are oriented as equatorial and axial, respectively. Other indications are provided from the strong cross peaks between the signals of isopropyl CH (H^h) and phenyl (Ph) protons, H^j and Hⁱ, H^a and H^f in the ¹H-¹H NOESY spectrum of **2a**. Moreover, it can be deduced that the *i*Pr substituent occupies an axial position on the nitrogen atom whose configuration is thus (*R*). This is most obvious from the NOESY and ¹H NMR spectra, where N-H shows a characteristic W-coupling with the equatorial methylene proton (⁴J(H^g,H^d) = 1.3 Hz), which is only possible in an equatorial arrangement of H on N.¹³ Another important cross peak appears in the NOESY spectrum between the signal of H^g and H^f indicating spatial vicinity for these protons, while a cross peak between the *i*Pr protons and H^f is absent. Accordingly, it can be stated that **2a** is present in a single chair conformation (Figure 3), i.e. the arrangement of ring alkyl substituents is equatorial-axial-axial moving from the phosphorus towards the nitrogen along the ligand backbone.†

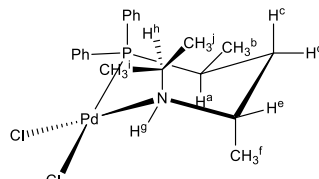
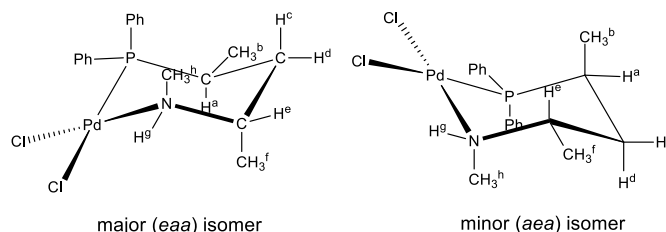
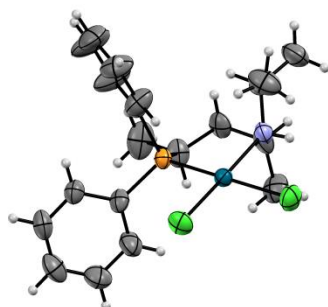


Figure 3. Structure of **2a**

In contrast to **2a**, compound **2b** with sterically less demanding N-Me substituents exists in two isomeric forms at room temperature in a molar ratio of 1.7-2.3 to 1 depending slightly on the NMR solvent used. Moreover, the composition remained unchanged in the temperature range of 243-315 K in CDCl₃ or upon standing at room temperature. The major isomer is stabilized in *eaa* conformation that can be deduced from the ¹H, ¹³C NMR (of the ring carbons) and NOESY ¹H-¹H correlation spectra. In this case similar characteristic couplings and crosspeaks, respectively, were found to those of compound **2a**. The minor isomer also adopts a chair conformation as indicated by the large ~30 Hz coupling of ³J(P,H^c)¹³ and the -15.8 Hz geminal ²J(H^c,H^d) coupling¹⁴ (Figure 4). Furthermore, the J(P-C) coupling constants of the minor isomer in the ¹³C NMR spectrum are similar to those of the major complex, except ²J(P-C^{methyl}) as expected. The observed ³J(P,H^b) coupling of 16.2 Hz is typical for an axial Me next to P.¹³ In the NOESY spectrum of the minor complex, cross peaks appear between the signals of H^b and H^e, and H^h protons and H^f. The vicinity of N-Me group causes a large upfield chemical shift of the equatorial Me-group (H^f) in the ¹H NMR spectrum. These together with the observed characteristic W-coupling between H^g and H^c on the ¹H NMR spectrum clearly prove that the Me substituent on the nitrogen atom occupies an axial position, whose configuration is thus (*S*). As a consequence, it can be stated the minor **2b** isomer exists in *aea* conformation (Figure 4).†

**Figure 4.** The observed conformers of **2b**

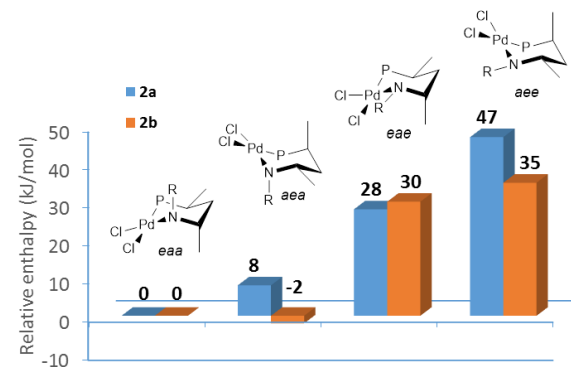
X-ray characterization of 2a. X-ray structure analysis of a single crystal grown by slow evaporation of the solvent from the solution of **2a** in acetone confirms in all respects the structural data deduced from the NMR spectra. The coordination sphere of the complex has the usual distorted square planar geometry (Figure 5).[‡] The Pd-Cl bond length *trans* to phosphorus ($2.371(3)$ Å) is somewhat longer than that *trans* to the nitrogen ($2.295(3)$ Å) reflecting the larger *trans* influence of the phosphine compared to the amine. Furthermore, a weak H-bond type interaction between the equatorially disposed NH and the *cis* chloride can further stabilize the conformation of the complex.

**Figure 5.** X-ray structure (ORTEP view at 50% probability level) of **2a**

DFT analysis for complexes 2a-b. In order to gain deeper insight into the thermodynamic stability of the possible chair conformations, density functional theory geometry optimizations were performed for complexes **2** using the CAM-B3LYP functional combination with the SDD basis set and pseudopotential for Pd as well as the 6-31G* basis set for the rest of the atoms. The enthalpy differences between the chair conformers are shown in Diagram 1.

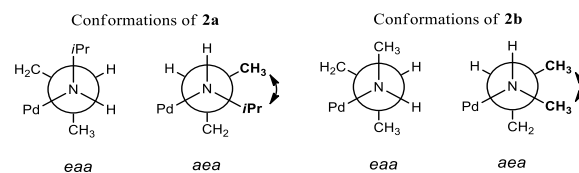
From the four possible stereoisomers of **2a** shown in Figure 2, the lowest-energy species is identical to the one observed experimentally both in solid and solution phases. The DFT calculations show that the enthalpy of the chelates containing the N-iPr group in axial position (*eaa* and *aea*) is lower (0 and 8 kJ/mol) compared to those of the equatorial derivatives (28 and 47 kJ/mol). The reason for the preference of the somewhat unexpected axial position of the N-iPr group is the smaller 1,2 inter-ligand interaction with the *cis* ligand (in this case a Cl atom) in the lower-energy species than in the others (Diagram 1).^{3a}

In compound **2b** the isomers with equatorial N-Me substituent also constitutes higher energy species (*eae* and *aea* isomers). However, in the case of complex **2b** the theoretical calculations forecast that both the *eaa* and *aea* (Diagram 1, 0 and -2 kJ/mol relative enthalpies, respectively) structures can form, where the N-substituent is in axial position (Figure 2). The formation of chelates containing only axial N-substituents underline the significance of 1,2 inter-ligand interactions in the complex formation processes.

**Diagram 1.** Calculated relative enthalpies of the chair structures of **2**

To substantiate this assumption we performed further DFT studies by removing the Cl substituents from **2a**. Indeed, the relative enthalpy difference (ΔH^0) between the *eaa* and *eae* conformations in this case is *ca.* 2 kJ/mol, much smaller than 28 kJ/mol found in the dichloro complex.

The DFT calculations also provide information on the preference of the *eaa* vs. the *aea* conformer in **2a**. In the *aea* conformer the torsion angle between the *iPr* and the adjacent ring Me group is approximately 60° (Figure 6). The steric interaction between the *synclinal* Me and *iPr* groups in this conformer is supposed to be significant. In addition, the isopropyl CH points toward the axial Ph placing the *iPr* methyl group in the close proximity of the backbone methyl substituent that increases the steric strain further between the two alkyl groups. In contrast to this, such interaction does not occur in the *eaa* conformer with antiperiplanar alkyl substituents. In order to support this explanation, we performed DFT studies on the *ae* and *aa* diastereomers of 1-isopropyl-2-methylcyclohexane as a simple model. The enthalpy of the *aa* isomer with *anti*-positioned 1,2-substituents is approximately 8 kJ/mol lower than that of the *ae* structure. However, in the case of 1,2-dimethylcyclohexane as a model compound for **2b**, the DFT calculations showed that the diaxial isomer is *ca.* 5 kJ/mol less stable than the *ea* structure. Therefore, in the *aea* isomer of **2b** the steric strain between the two Me groups in *synclinal* position is not remarkable compared to that in **2a**. These observations clearly prove the fundamental role of the N-substituents in determining the stereocontrol in the complex formation.

**Figure 6.** Newman projections of *eaa* and *aea* isomers

Analysis of complexes 3a-b. The ^1H and $^{31}\text{P}\{^1\text{H}\}$ NMR spectra of the substrate complex **3a** (Figure 7) revealed two isomers at room temperature with a molar ratio of 4-7 to 1 depending moderately and reproducibly on the NMR solvent used. Furthermore, the composition remained the same in d_6 -acetone cooling down to 193 K or upon standing at room temperature in each of the solvents. The ratio of major isomer was the highest in d_6 -acetone and the lowest in CD_2Cl_2 by using these solvents and CDCl_3 . The structure analysis of **3a** by ^1H , $^1\text{H}-^1\text{H}$ COSY and NOESY techniques proved that the chelate ring also adopts *eaa* conformation both in the major and minor isomers: similar $^3J(\text{P},\text{H})$, $^3J(\text{H},\text{H})$ and $^2J(\text{H},\text{H})$ couplings appear in the appropriate protons as in complex **2a**. The major and

minor isomers are assigned to the *exo* and *endo* complexes that can be evidenced by referring to analogies with ^1H chemical shifts from earlier studies¹⁵ or by the observed inter-ligand cross peaks in the ^1H - ^1H NOESY spectrum. These cross peaks appear, for example, between H^{i} and H^{m} in the *endo* and between H^{i} and H^{m} , H^{i} and H^{i} in the *exo* isomer (Figure 7). The formation of the theoretically possible *syn-anti* isomers can be excluded, since in both species $\text{H}^{\text{k}}\text{-H}^{\text{m}}$ crosspeaks appear as an evidence for the *syn-syn* geometry.[†] In accordance with the structure of **3a** in solution, DFT calculations also proved that the *exo* isomer is the lower energy species.[†] As it was surmised for Pd-diphenylallyl complexes of phosphine-oxazoline (PHOX) ligands¹⁶, the preference of the *exo* isomer over the *endo* originates from the *face* positioned equatorial P-Ph group which repels the substituent at C1 atom of the allyl group.¹⁷ In our case the same inter-ligand interaction could be proposed as a dominating factor determining the coordination mode of the allylic moiety.

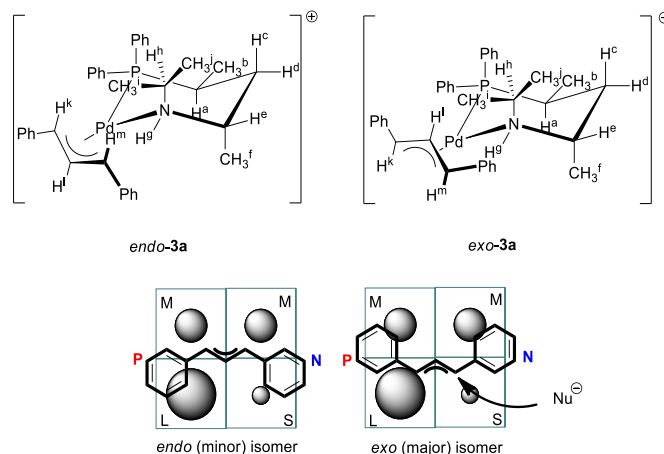


Figure 7. *Endo* and *exo* isomers of **3a**; quadrant diagram for η^3 -diphenylallyl complexes: hydrogen is the small group (S), the *iPr* and the axial, edge positioned Ph are considered medium groups (M), and the equatorial Ph with face position is considered large (L).

In contrast to that, complex **3b** exhibits four isomers in solution in a molar ratio of 2.6/1.6/1/5.6 according to the ^1H and ^{31}P NMR signals in CD_2Cl_2 at room temperature. In other words the number of the complex species is doubled compared to that in the dichloro complex **2b** (~2:1 isomeric molar ratio). Therefore, it is reasonable to assume that the four isomeric complex species can be assigned as the *endo* and *exo* isomers of both the *eaa* and *aea* chelate conformers.

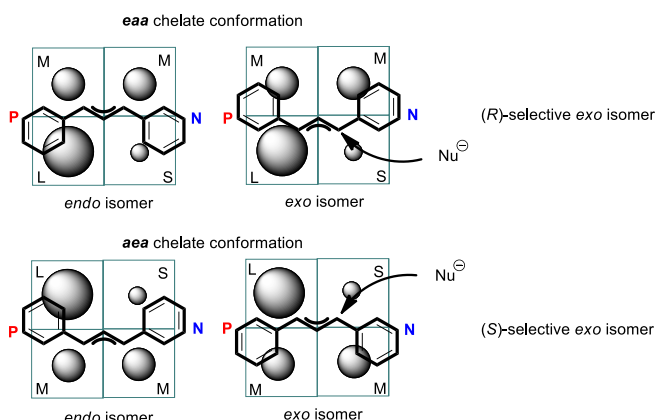
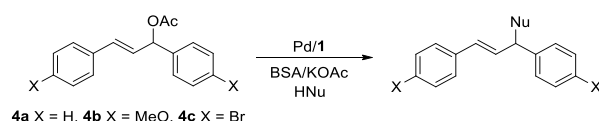


Figure 8. Possible isomeric species of **3b**; the more abundant and more reactive *exo* isomers of *eaa* and *aea* conformations have the opposite selectivities

Catalytic studies

Ligand **1a** and **1b** were tested in the palladium-catalyzed asymmetric allylic alkylation of benchmark substrates (**4a-c**) by using several nucleophiles (Scheme 2).

The catalyst modified by **1a** provided excellent activities and *ees* (Table 1). The reactions completed in 1 h in each case at a substrate/catalyst molar ratio of 100. The best enantioselectivity (96%) was obtained by using acetylacetone as nucleophile. The products of the reactions had predominantly (*R*) configuration. This product distribution suggests that the major product enantiomer is formed upon the nucleophilic attack on the allylic termini *trans* to the phosphorus in the *exo* isomer or *trans* to the nitrogen in the *endo* species (Figure 7). Based on our results¹⁸ and other studies on Pd-P,N systems,¹⁹ it can be stated that stereoelectronically, the Pd-allyl terminus opposite to the more powerful acceptor atom (phosphorus) will be more susceptible to cleavage as a result of nucleophilic attack. Accordingly, it seems to be obvious that the nucleophile attacks preferentially the allylic carbon *trans* to the phosphorus in the *exo* isomer.



Scheme 2. Asymmetric allylic alkylation by using ligand **1a**

The advantage of the stereoselective coordination of N in asymmetric alkylation was clearly proven by using ligand **1b** instead of **1a**. The reaction of substrate **4a** with malonate nucleophiles resulted in low enantioselectivities (up to 30%, Table 1, entries 7-9). It can be explained by the presence of four substrate complex isomers enhancing the number of competitive catalytic pathways. Based on the assumptions that the coordination mode of the allylic moiety is governed by the same interactions as in **3a** and that the reaction occurs with a preferential *trans*-to-P nucleophilic attack of the *exo* isomer, it is evident that the *eaa* conformation results in the formation of (*R*) prevailing enantiomer in contrast to *aea* that provides the product with (*S*)-selectivity (Figure 8). Indeed, the observed low enantioselectivity is the result of at least two competing reaction pathways. Since the number and ratio of the possible chelate conformers is strongly affected by the nature of the nitrogen substituent it can be concluded that both the stereoselective coordination of the nitrogen and the ring conformation are responsible for the high *exo/endo* ratio that have a profound effect (Table 1) on the enantioselectivity in asymmetric alkylation reactions.

The role of the ligand/palladium molar ratio was also investigated as an important factor for influencing enantioselectivity. Gradually increasing the ratio of **1a** to Pd from 1 to 6 in the reaction of diphenylallyl acetate with dimethyl malonate, the enantioselectivity steadily decreases from a value of 94% to 56%. This observation can be explained by the formation of a *bis*-P-ligand complex in the presence of an excess amount of ligand and thus in the absence of a chelate with stereogenic nitrogen, which causes a decline in enantioselectivity.^{20,5b}

Table 1. Asymmetric allylic alkylation by using ligand **1a** and **1b**

entry	ligand	substrate	HNu	ee (%)
1	1a	4a	CH(COOMe) ₂	94
2	1a	4b	CH(COOMe) ₂	94
3	1a	4c	CH(COOMe) ₂	92
4	1a	4a	CH(COMe) ₂	96
5	1a	4a	CH(COOEt) ₂	92
6	1a	4a	CH(COOBn) ₂	94
7	1b	4a	CH(COOMe) ₂	24
8	1b	4a	CH(COOEt) ₂	30
9*	1b	4a	CH(COOBn) ₂	28

Reaction conditions: catalyst prepared *in situ* from 0.5 mol% of $[(\eta^3\text{-C}_3\text{H}_5)\text{PdCl}]_2$ and 1 mol% of chiral ligand; substrate 1.25 mmol; solvent 10 mL of CH_2Cl_2 ; KOAc 7 mg; temperature RT; reaction time 1 h. The conversion was complete in each case. Prevailing configuration of the products: (*R*). *Conversion is 70%.

Experimental

General experimental details. All manipulations were carried out under argon using Schlenk techniques. Solvents were purified, dried and deoxygenated by standard methods. Compounds **1a** and **1b**,¹⁰ $[\text{Pd}(\text{COD})\text{Cl}_2]$ ²¹ and $[\text{Pd}(\text{PhCHCHCHPh})\text{Cl}_2]$ ²² were prepared according to literature methods. All other starting materials were purchased from Sigma Aldrich. ³¹P{¹H}-, ¹³C{¹H}- and ¹H-NMR spectra including ¹H-¹H COSY and NOESY measurements were recorded on a Bruker Avance 400 spectrometer (NMR Laboratory, University of Pannonia) operating at 161.98, 100.61 and 400.13 MHz respectively. The ¹H couplings were determined by using gNMR 6.0 NMR simulation program written by P. H. M. Budzelaar (Copyright: 2006 IvorySoft). ESI mass spectra were recorded on an Agilent 1100 LC/MSD SL Quadrupole mass spectrometer (Department of Earth and Environmental Science, University of Pannonia). X-ray data for compound **2a** were collected on a Bruker-Nonius MACH3 diffractometer (Laboratory for X-ray diffraction, University of Debrecen). Theoretical calculations were performed by using the CAM-B3LYP functional combination with the SDD basis set and pseudopotential for Pd as well as the 6-31G* basis set for the rest of the atoms.

Synthesis and characterization of complex **2a.** Ligand **1a** (109 mg, 0.3502 mmol) dissolved in CH_2Cl_2 (5 mL) was added dropwise to a solution of $[\text{Pd}(\text{COD})\text{Cl}_2]$ (100 mg, 0.3502 mmol) in CH_2Cl_2 (5 mL). The resulting orange solution was stirred for 20 min, filtered through a short pad of celite and concentrated to *ca.* 2 mL. The solution was then treated with ether (10 mL) to precipitate an orange powder that was filtered and washed with ether (5 mL) to give 153 mg of **2a**. Yield: 90%. mp. 192–195 °C. ¹H NMR (400 MHz, CD_2Cl_2): δ = 8.12–7.36 (m, 10H, aromatic, wherein 8.09 m, 2H; 7.67 m, 1H; 7.60 m, 2H; 7.48 m, 1H; 7.41 m, 4H), 4.52 (br d, J = ~10.2 Hz (³J(H^b,H^g) = 12.7 Hz, ³J(H^e,H^g = 3.0 Hz.), 1H, H^g), 3.21 (m, ³J(H^g,H^e) = 3.0 Hz, ³J(H^c,H^e) = 3.0 Hz, ³J(H^d,H^g) = 3.9 Hz, ³J(H^f,H^g) = 6.6 Hz, 1H, H^e), 2.63 (m, ³J(H^g,H^h) = 12.7 Hz, ³J(H^{CH₃(iPr)},H^h) = 6.2 Hz, ³J(H^{CH₃(iPr)},H^h) = 6.6 Hz, 1H, H^h), 2.585 (m, ²J(P,H^a) = 10.6 Hz, ³J(H^c,H^a) = 13.4 Hz, ³J(H^d,H^a) = 3.9 Hz, ³J(H^b,H^a) = 7.2 Hz, 1H, H^a), 2.27 (dddd, ³J(P,H^c) = 7.6 Hz, ³J(H^a,H^c) = 13.4 Hz, ³J(H^e,H^c) = 3.0 Hz, ²J(H^d,H^c) = -15.9 Hz, 1H, H^c), 1.96 (ddtd, ³J(P,H^d) = 35.1 Hz, ³J(H^a,H^d) = 3.9 Hz, ³J(H^e,H^d) = 3.9 Hz, ²J(H^c,H^d) = -15.9 Hz, ⁴J(H^g,H^d) = 1.3 Hz, 1H, H^d) 1.86 (br d, ³J(H^e,H^f) = 6.6 Hz, 3H, H^f), 1.46 (d, ³J(H^h,H^{CH₃(iPr)}) = 6.6 Hz, 3H, diast. CH₃(iPr)), 1.20 (dd, ³J(P,H^b) = 12.5 Hz, ³J(H^a,H^b) = 7.2 Hz, 3H, H^b), 1.09 (d,

³J(H^h,H^{CH₃(iPr)}) = 6.2 Hz, 3H, diast. CH₃(iPr)). In CDCl_3 a very similar spectrum was obtained with somewhat worse resolution. ¹³C NMR (101 MHz, CDCl_3): δ = 134.19–125.27 (12C, aromatics), 51.61 (s, 1C, CH(iPr)), 48.93 (d, ³J(P,C) = 3.9 Hz, 1C, CH(N)), 33.77 (d, ²J(P,C) = 0.9 Hz, 1C, CH₂), 25.19 (s, 1C, diast. CH₃(iPr)), 25.00 (d, ¹J(P,C) = 27.3 Hz, 1C, CH(P)), 21.33 (s, 1C, diast. CH₃(iPr)), 20.84 (s, 1C, CH₃(CHN)), 16.60 (d, ²J(P,C) = 8.4 Hz, 1C, CH₃(CHP)). ³¹P NMR (162 MHz, CD_2Cl_2): δ = 22.81 (s). ESI mass spectrum: m/z 455.8 [M – Cl]⁺, 419.0 [M – 2Cl]⁺ (calculated 456.07 [M – Cl]⁺, 419.1 [M – 2Cl]⁺). IR (KBr, cm⁻¹): 528, 686, 745, 1058, 1097, 1386, 1434, 2875, 2928, 2974, 3053, 3191 (s, v(NH)).

Synthesis and characterization of **2b.** Ligand **1b** (90 mg, 0.3502 mmol) dissolved in CH_2Cl_2 (5 mL) was added dropwise to a solution of $[\text{Pd}(\text{COD})\text{Cl}_2]$ (100 mg, 0.3502 mmol) in CH_2Cl_2 (5 mL). The resulting orange solution was stirred for 20 min, filtered through a sort pad of celite and concentrated to *ca.* 2 mL. The solution was then treated with ether (10 mL) to precipitate an orange powder that was filtered and washed with ether (5 mL) to give 140 mg of **2b**. Yield: 87%. mp. 202–205 °C. *eeaa* (major) isomer of **2b**: ¹H NMR (400 MHz, CD_2Cl_2): δ = 8.21–7.32 (m, 10H, aromatic, overlapped by the aromatic signals of the *aea* isomer), 4.77 (br s, 1H, H^g), 2.83 (m, 1H, H^e), 2.61 (dd, J = 6.6 Hz, J = 0.9 Hz, 3H, H^h), 2.58 (m, 1H, H^a, overlapped with minor H^a), 2.18 (m, 1H, H^c, overlapped with minor H^d), 1.84 (ddtd, ³J(P,H^d) = 35 Hz, ²J(H^c,H^d) = -15.9 Hz, ³J(H^a,H^d) = 3.4 Hz, ³J(H^e,H^d) = 3.4 Hz, ⁴J(H^g,H^d) = 1.2 Hz, 1H, H^d, partly overlapped with minor H^c), 1.65 (d, ³J(H^e,H^f) = 6.6 Hz, 3H, H^f), 1.16 (dd, ³J(P,H^b) = 12.5 Hz, ³J(H^a,H^b) = 7.3 Hz, 3H, H^b), overlapped with minor H^f). ¹³C NMR (101 MHz, CD_2Cl_2): δ = 136.1–124.5 (12C, aromatic), 55.25 (d, ³J(P,C) = 3.9 Hz, 1C, CH(N)), 41.15 (s, 1C, CH₃(N)), 33.79 (d, ²J(P,C) = 3.2 Hz, 1C, CH₂), 23.40 (d, ¹J(P,C) = 27.3 Hz, 1C, CH(P)), 19.92 (s, 1C, CH₃(CHN)), 17.01 (d, ²J(P,C) = 8.3 Hz, 1C, CH₃(CHP)). ³¹P NMR (162 MHz, CD_2Cl_2): δ = 21.61 (s). *aea* (minor) isomer of **2b**: ¹H NMR (400 MHz, CD_2Cl_2): 8.21–7.32 (m, 10H, aromatic, overlapped with the aromatic signals of the *aea* isomer), 4.59 (br s, 1H, H^g), 3.43 (m, 1H, H^e), 2.58 (m, 1H, H^a, overlapped with major H^a), 2.23 (dd, J = 6.3 Hz, J = 1.2 Hz, 3H, H^h), 2.11 (m, 1H, H^d, partly overlapped with major H^c), 1.75 (dddt, ³J(P,H^c) = ~30 Hz, ²J(H^c,H^d) = -15.8 Hz, ³J(H^e,H^c) = 4.9 Hz, ³J(H^a,H^c) = 1.6 Hz, ³J(H^g,H^c) = 1.6 Hz, 1H, H^c, partly overlapped with major H^d), 1.22 (dd, ³J(P,H^b) = 16.2 Hz, ³J(H^a,H^b) = 7.2 Hz, 3H, H^b), 1.12 (d, ³J(H^e,H^f) = 7.0 Hz, 3H, H^f, overlapped with major H^b). ¹³C NMR (101 MHz, CD_2Cl_2): δ = 136.1–124.5 (12C, aromatic), 55.14 (d, ³J(P,C) = 3.8 Hz, 1C, CH(N)), 41.14 (s, 1C, CH₃(N)), 33.93 (d, ²J(P,C) = 1.9 Hz, 1C, CH₂), 25.53 (d, ¹J(P,C) = 29.2 Hz, 1C, CH(P)), 20.90 (s, 1C, CH₃(CHN)), 16.05 (d, ²J(P,C) = 2.5 Hz, 1C, CH₃(CHP)). ³¹P NMR (162 MHz, CD_2Cl_2): δ = 27.29 (s). ESI mass spectrum: m/z 390.1 [M – H – 2Cl]⁺ (calculated 390.07 [M – H – 2Cl]⁺). IR (KBr, cm⁻¹): 510, 538, 606, 692, 748, 1046, 1101, 1382, 1436, 2873, 2926, 2966, 3052, 3185 and 3212 (s, v(NH)).

Synthesis and characterization of complex **3a.** Ligand **1a** (63.4 mg, 0.2022 mmol) dissolved in CH_2Cl_2 (5 mL) was added dropwise to a suspension of $[\text{Pd}(\eta^3\text{-PhCHCHCHPh})\text{Cl}_2]$ (67.8 mg, 0.1011 mmol) in CH_2Cl_2 (5 mL). The resulting orange solution was stirred for 20 min and then AgBF₄ (39.4 mg, 0.2022 mmol) was added. The reaction mixture was stirred for 1 h, filtered through a sort pad of celite and concentrated to *ca.* 2 mL. The solution was then treated with ether (10 mL) to precipitate an orange powder that was filtered and washed with ether (5 mL) to give 127 mg of **3a**. Yield: 87%. mp. 101–105 °C. ¹H NMR (400 MHz, CD_2Cl_2): *exo*-**3a**: δ = 7.73–6.75 (m (partly overlaps with the analogous *endo* signal), 20H, aromatic), 6.58 (dd (overlap with the analogous *endo* signal), ³J(H^k,H^l) = 11.1 Hz, ³J(H^m,H^l) = 13.5 Hz, 1H, H^l), 5.64 (dd, ³J(P,H^m) = 7.9 Hz, ³J(H^l,H^m) 1H, H^m), 4.24 (d, ³J(H^l,H^k) = 11.1 Hz, 1H, H^k),

3.46 (br m, $^3J(H^e,H^e)$ ~ 3.0 Hz, $^3J(H^c,H^e)$ = 3.0 Hz, $^3J(H^d,H^e)$ = 3.2 Hz, $^3J(H^f,H^e)$ = 6.5 Hz, 1H, H^e), 2.84 (m, $^2J(P,H^a)$ ~ 7.5 Hz, $^3J(H^c,H^a)$ ~ 11.6 Hz, $^3J(H^d,H^a)$ = 3.2 Hz, $^3J(H^b,H^a)$ = 7.2 Hz, 1H, H^a), 2.59 (m, $^3J(H^g,H^b)$ = 12.0 Hz, $^3J(H^{CH_3(iPr)},H^b)$ = 6.1 Hz, $^3J(H^{CH_3(iPr)},H^b)$ = 6.4 Hz, 1H, H^b), 1.95 (m (partly coincides with the analogous *endo* signal), $^3J(P,H^c)$ ~ 13.5 Hz, $^3J(H^a,H^c)$ ~ 11.6 Hz, $^3J(H^e,H^c)$ = 3.0 Hz, $^2J(H^d,H^c)$ = -15.9 Hz, 1H, H^c), 1.76 (ddt (partly overlap with the analogous *endo* signal), $^3J(P,H^d)$ = 36.9 Hz, $^3J(H^a,H^d)$ = 3.2 Hz, $^3J(H^e,H^d)$ = 3.2 Hz, $^2J(H^c,H^d)$ = -15.9 Hz, $^4J(H^g,H^d)$ < 1 Hz, 1H, H^d) 1.75 (br, d, $^3J(H^e,H^f)$ = 6.5 Hz, $^4J(H^g,H^f)$ < 1 Hz), 3H, H^f), 1.59 (br d, ~ 11.3 Hz, $^3J(H^h,H^g)$ = 12.0 Hz, $^3J(H^e,H^g)$ ~ 3.0 Hz) 1H, H^g), 1.15 (dd, $^3J(P,H^b)$ = 11.1 Hz, $^3J(H^a,H^b)$ = 7.2 Hz, 3H, H^b), 0.73 (d, $^3J(H^h,H^{CH_3(iPr)})$ = 6.1 Hz, 3H, diast. CH₃(iPr)), 0.70 (d, $^3J(H^h,H^{CH_3(iPr)})$ = 6.4 Hz, 3H, diast. CH₃(iPr)). $^{13}C\{^1H\}$ NMR (101 MHz, CD₂Cl₂): δ = 137.35-116.38 (m, 24C, aromatic partly overlaps with analogous *endo* signals) 110.95 (d, $^2J(P,C)$ = 4.4 Hz, 1C, CH^l), 97.12 (d, $^2J(P,C)$ = 20.3 Hz, 1C, CH^m), 72.57 (d, $^2J(P,C)$ = 5.0 Hz, 1C, CH^k), 50.53 (s, 1C, CH(iPr)), 50.39 (d, $^3J(P,C)$ = 2.4 Hz, 1C, CH(N)), 33.34 (d, $^2J(P,C)$ = 3.5 Hz, 1C, CH₂), 26.83 (d, $^1J(P,C)$ = 19.6 Hz, 1C, CH(P)), 23.71 (br s, $^4J(P,C)$ < 0.8 Hz 1C, CH₃(CHN)), 20.77 (s, 1C, diast. CH₃(iPr)), 20.65 (s, 1C, diast. CH₃(iPr)), 17.31 (d, $^2J(P,C)$ = 8.4 Hz, 1C, CH₃(CHP)). ^{31}P NMR (162 MHz, CD₂Cl₂): δ = 25.09 (s). *endo*-3a: δ = 7.91-6.46 (m (partly overlaps with the analogous *exo* signal, wherein 7.86 m, 2H, 6.49 m 2H), 20H, aromatic), 6.58 (dd (overlap with the analogous *exo* signal), $^3J(H^k,H^l)$ = 12.5 Hz, $^3J(H^m,H^l)$ = 11.8 Hz, 1H, H^l), 5.07 (dd, $J(P,H^m)$ = 10.3 Hz, $^3J(H^l,H^m)$ = 11.8 Hz, 1H, H^m), 4.99 (d, $^3J(H^l,H^k)$ = 12.5 Hz, 1H, H^k), 3.24 (br m, $^3J(H^g,H^e)$ ~ 3.0 Hz, $^3J(H^e,H^e)$ = 3.0 Hz, $^3J(H^d,H^e)$ = 3.6 Hz, $^3J(H^f,H^e)$ = 6.9 Hz, 1H, H^e), 2.74 (m, $^3J(H^g,H^b)$ ~ 14.0 Hz, $^3J(H^{CH_3(iPr)},H^b)$ = 6.1 Hz, $^3J(H^{CH_3(iPr)},H^b)$ = 6.5 Hz, 1H, H^b), 2.40 (m, $^2J(P,H^a)$ ~ 10.0 Hz, $^3J(H^c,H^a)$ ~ 11.6 Hz, $^3J(H^d,H^a)$ = 3.6 Hz, $^3J(H^b,H^a)$ = 7.2 Hz, 1H, H^a), 2.04 (m (partly coincides with the analogous *exo* signal), $^3J(P,H^c)$ ~ 12.0 Hz, $^3J(H^a,H^c)$ ~ 11.6 Hz, $^3J(H^e,H^c)$ ~ 3.0 Hz, $^2J(H^d,H^c)$ = -16.0 Hz, 1H, H^c), < 1.77 (~ddtd (only a portion is visible as signal coincides with the analogous *exo* signal, H^f and H^g), $^3J(P,H^d)$ covered (35 Hz used for simulation), $^3J(H^a,H^d)$ ~ 3.6 Hz, $^3J(H^e,H^d)$ ~ 3.6 Hz, $^2J(H^c,H^d)$ ~ 16.0 Hz, $^4J(H^g,H^d)$ ~ 1.2 Hz, 1H, H^d), 1.52 (br d, $^3J(H^b,H^g)$ ~ 14.0 Hz, $^3J(H^e,H^g)$ ~ 3.0 Hz 1H, H^g), 1.36 (d, $^3J(H^h,H^{CH_3(iPr)})$ = 6.5 Hz, 3H, diast. CH₃(iPr)), 1.15 (d, $^3J(H^e,H^f)$ = 6.9 Hz, 3H, H^f), 1.05 (dd, $^3J(P,H^b)$ = 11.0 Hz, $^3J(H^a,H^b)$ = 7.2 Hz, 3H, H^b), 0.92 (d, $^3J(H^h,H^{CH_3(iPr)})$ = 6.1 Hz, 3H, diast. CH₃(iPr)). $^{13}C\{^1H\}$ NMR (101 MHz, CD₂Cl₂): Alkyl region is tentatively assigned by the analogy with 2a, δ = 137.35-116.38 (m, 24C, aromatic partly overlaps with analogous *exo* signals), 108.11 (d, $^2J(P,C)$ = 6.8 Hz, 1C, CH^l), 90.49 (d, $^2J(P,C)$ = 21.6 Hz, 1C, CH^m), 77.86 (d, $^2J(P,C)$ = 4.4 Hz, 1C, CH^k), C^h is probably buried by the analogous signal of *exo*-3a, 50.32 (d, $^3J(P,C)$ = 2.2 Hz, 1C, CH(N)), 33.12 (d, $^2J(P,C)$ = 5.0 Hz, 1C, CH₂), 26.26 (d, $^1J(P,C)$ = 20.3 Hz, 1C, CH(P)), 25.66 (d, $^4J(P,C)$ = 1.2 Hz, 1C, CH₃(CHN)), 23.71 (s, 1C, diast. CH₃(iPr)), 21.30 (s, 1C, diast. CH₃(iPr)), 17.66 (d, $^2J(P,C)$ = 8.0 Hz, 1C, CH₃(CHP)). ^{31}P NMR (162 MHz, CD₂Cl₂): δ = 27.98 (s). ESI mass spectrum: m/z 611.8 [M - BF₄]⁺, 419.0 [M - diphenylallyl - BF₄]⁺ (calculated 612.2 [M - BF₄]⁺, 419.1 [M - diphenylallyl - BF₄]⁺). IR (KBr, cm⁻¹): 518, 697, 754, 1059, 1384, 1436, 1457, 1489, 2871, 2928, 2960, 3026, 3050, 3225 (s, v(NH)).

Synthesis and characterization of complex 3b. Ligand **1b** (57.7 mg, 0.2022 mmol) dissolved in CH₂Cl₂ (5 mL) was added dropwise to a suspension of [Pd(η^3 -PhCHCHCHPh)Cl]₂ (67.8 mg, 0.1011 mmol) in CH₂Cl₂ (5 mL). The resulting orange solution was stirred for 20 min and then AgBF₄ (39.4 mg, 0.2022 mmol) was added. The reaction mixture was stirred for 1 h, filtered through a short pad of celite and concentrated to ca. 2 mL. The solution was then treated with ether (10 mL) to precipitate an orange powder that was filtered and washed with ether (5 mL) to give 125 mg of **3b**. Yield: 92%. mp. 92-95 °C. 1H NMR (400 MHz, CD₂Cl₂): δ = 8.02-6.70 (m,

aromatic protons for the four isomers), 6.6-6.5 (m, internal allylic protons for the four isomers, overlapped), 5.87 (dd, $J(P,H)$ = 12.9 Hz, $J(H,H)$ = 9.1 Hz, terminal allylic H *trans* to P for one isomer), 5.53 (dd, $J(P,H)$ = 13.0 Hz, $J(P,H)$ = 8.0 Hz, terminal allylic H *trans* to P for one isomer), 5.41 (dd, $J(P,H)$ = 13.1 Hz, $J(P,H)$ = 8.1 Hz terminal allylic proton *trans* to P for one isomer, overlapped), 5.40 (dd, $J(P,H)$ = 11.9 Hz, $J(P,H)$ = 9.6 Hz terminal allylic proton *trans* to P for one isomer, overlapped), 4.95 (d, $^3J(H,H)$ = 12.0 Hz, terminal allylic proton *trans* to N for one isomer), 4.70 (d, $^3J(H,H)$ = 11.9 Hz, terminal allylic proton *trans* to N for one isomer), 4.26 (d, $^3J(H,H)$ = 11.4 Hz, terminal allylic proton *trans* to N for one isomer), 4.12 (d, $^3J(H,H)$ = 11.2 Hz, terminal allylic proton *trans* to N for one isomer), 3.71-0.91 (m, aliphatic protons for the four isomers). (Three of the N-methyl signals can be tentatively assigned: 2.65 (d, J = 6.2 Hz, for one isomer), 2.12 (d, J = 6.4 Hz, for one isomer), 2.00 (d, J = 6.2 Hz, for one isomer).) ^{31}P NMR (162 MHz, CD₂Cl₂): δ = 27.28 (s), 24.1 % P; 26.52 (s), 14.8 % P; 26.17 (s), 9.2 % P; 25.30 (s), 51.9 % P. ESI mass spectrum: m/z 585.6 [MH - BF₄]⁺, 299.0 [M - **1b** - BF₄]⁺ (calculated 585.17 [MH - BF₄]⁺, 299.1 [M - **1b** - BF₄]⁺). IR (KBr, cm⁻¹): 524, 637, 693, 755, 1030, 1149, 1261, 1437, 1462, 1490, 2868, 2929, 2958, 3048, 3230 (s, v(NH)).

Catalytic experiments. A degassed solution of [Pd(η^3 -C₃H₅)Cl]₂ (2.28 mg, 0.00625 mmol) and ligand **1a** or **1b** (0.0125 mmol in the case of 1/1 Pd/ligand molar ratio) in the corresponding solvent (10 mL) was stirred for 30 min, then the substrate (1.25 mmol) was added and the solution was stirred for a further 15 min. Subsequently, the nucleophile (3.75 mmol), potassium acetate (7 mg) and *N,O*-bis(trimethylsilyl)-acetamide (0.91 mL, 3.75 mmol) were added and the reaction mixture was stirred at room temperature. After being stirred, it was diluted with ether (10 mL) and a saturated aqueous solution of NH₄Cl was added. The mixture was extracted with ether (3x10 mL) and the extract dried over MgSO₄. The solution was then passed through a short pad of silica and was eluted with ether. The solvent was then evaporated and the residue dissolved in a mixture of *n*-hexane/2-propanol. The enantioselectivity and the conversion were determined by chiral HPLC (Column: Kromasil 3-AmyCoat, 4.6x150 mm). Retention times for the enantiomers of allylation products: (E)-dimethyl 2-(1,3-diphenylallyl)malonate (eluent: *n*-hexane/2-propanol 85/15 flow rate: 0.5 mL/min, λ : 254 nm) 10.6 and 13.7 min; (E)-diethyl 2-(1,3-diphenylallyl)malonate (eluent: *n*-hexane/2-propanol 85/15 flow rate: 0.5 mL/min, λ : 254 nm) 8.4 and 10.4 min; (E)-dibenzyl 2-(1,3-diphenylallyl)malonate (eluent: *n*-hexane/2-propanol 85/15 flow rate: 0.5 mL/min, λ : 254 nm) 16.2 and 19.7 min; (E)-3-(1,3-diphenylallyl)pentane-2,4-dione (eluent: *n*-hexane/2-propanol 95/5 flow rate: 0.5 mL/min, λ : 254 nm) 12.5 and 13.2 min; (E)-dimethyl 2-(1,3-bis(4-methoxyphenyl)allyl)malonate (eluent: *n*-hexane/2-propanol 85/15 flow rate: 0.5 mL/min, λ : 254 nm) 23.3 and 39.6 min; (E)-dimethyl 2-(1,3-bis(4-bromophenyl)allyl)malonate (eluent: *n*-hexane/2-propanol 85/15 flow rate: 0.5 mL/min, λ : 254 nm) 18.8 and 28.4 min.

Conclusions

In conclusion, we have shown that a modular P,N ligand based on a chiral pentane-2,4-diyl backbone with a stereogenic nitrogen atom reacts with palladium(II)-complexes to form a conformationally and configurationally stable species. The chelate rings of **1a** in complexes with Pd are stabilized in the same single chair structure displaying the alkyl substituents in equatorial-axial-axial (*eaa*) positions, moving from the phosphorus to the nitrogen along the ligand backbone. In contrast, complexes of ligand **1b** were observed in two chelate conformations showing the alkyl substituents both in equatorial-axial-axial (*eaa*) and in axial-equatorial-axial positions

(aea). X-ray crystallography, various NMR techniques and quantum chemical calculations allowed us to rationalize the preferential formation of the conformers on a structural basis. The stereoselective coordination of the ligand is governed by (i) the inter-ligand interaction between the N-alkyl group and the *cis* Pd-substituent, and (ii) by the torsional strain between N-alkyl and the adjacent methyl group in the Pd-complexes. The structure elucidation of these Pd(P-N) chelates shows the essential role of stereoselective coordination in asymmetric allylic alkylations as reflected by, the observed excellent activities and enantioselectivities (up to 96%) using **1a** as ligand. Thus, we have unambiguously proven that beside the chiral backbone and the electronic differences in the donor atoms of the chelate, the stereoselective coordination of the nitrogen can also play an important role in efficient asymmetric catalysis.

The latter highlights the fact that apparently “minor” but carefully chosen changes in the structure of the catalysts can dramatically improve their performances and also broaden the scope of the catalyst design, which can be taken as a rewarding justification of research efforts in this direction.

Acknowledgements

We thank Mr Béla Édes for skilful assistance in analytical measurements and synthetic experiments. The research was supported by the EU and co-financed by the European Social Fund under the project ENVIKUT (TÁMOP-4.2.2.A-11/1/KONV-2012-0043). The research was also supported by the ‘National Excellence Program’ in the framework of the project TÁMOP-4.2.4.A/2-11-2012-0001 and by the Hungarian Scientific Research Fund (OTKA K108966 and OTKA K115539).

Notes and references

[‡] X-Ray structural analysis: M = 490.70, orthorhombic, a = 10.8906 (3), b = 1.9745 (3), c = 16.810 (8) Å, U = 2175.36 (13) Å³, T = 293 K, space group P212121 (no.19), Z = 4, 2294 reflections measured. The final wR(F2) was 0.112 (all data).

- 1 (a) Bayardon, J. and Jugé, S. (2012) P-Chiral Ligands, in Phosphorus(III) Ligands in Homogeneous Catalysis: Design and Synthesis (eds P. C. J. Kamer and P. W. N. M. van Leeuwen), John Wiley & Sons, Ltd, Chichester, UK. (b) Thaler, T.; Guo, L.-N.; Steib, A. K.; Raducan, M.; Karaghiosoff, K.; Mayer, P.; Knochel, P. *Org. Lett.*, **2011**, *13*, 3182. (c) Lang, F., Li, D., Chen, J., Chen, J., Li, L., Cun, L., Zhu, J., Deng, J. and Liao, J. *Adv. Synth. Catal.*, **2010**, *352*, 843. (d) Malacea, R.; Daran, J.-C.; Poli, R.; Manoury, E. *Tetrahedron: Asymmetry* **2013**, *24*, 612. (e) Cheng, H.-G.; Lu, L.-Q.; Wang, T.; Chen, J.-R.; Xiao, W.-J. *Chem. Commun.* **2012**, *48*, 5596.
- 2 (a) Walsh, P. J.; Lurain, A. E.; Balsells, J. *Chem. Rev.* **2003**, *103*, 3297. (b) Pelz, K. A.; White, P. S.; Gagné, M. R. *Organometallics* **2004**, *23*, 3210.
- 3 (a) Cerasino, L.; Williams, K. M.; Intini, F. P.; Cini, R.; Marzilli, L. G.; Natile, G. *Inorg. Chem.* **1997**, *36*, 6070. (b) Rafii, E.; Dassonneville, B.; Heumann, A. *Chem. Commun.* **2007**, *583*. (c) Eckert, P. K.; Gessner, V. H.; Knorr, M.; Strohmann, C. *Inorg. Chem.* **2012**, *51*, 8516. (d) de Renzi, A.; Morelli, G.; Scalzone, M. *Inorg. Chim. Acta* **1982**, *65*, L119.
- 4 (a) Gavrilov, K. N.; Polosukhin, A. I. *Russ. Chem. Rev.* **2000**, *69*, 661. (b) Stepanova, V. A.; Smoliakova, I. P. *Curr. Org. Chem.* **2012**, *16*, 2893. (c) Carroll, M. P.; Guiry, P. J. *Chem. Soc. Rev.* **2014**, *43*, 819.
- 5 (a) Albinati, A.; Lanza, F.; Berger, H.; Pregosin, P. S.; Rüegger,

- H.; Kunz, R. W. *Inorg. Chem.* **1993**, *32*, 478. (b) Andrieu, J.; Camus, J.-M.; Dietz, J.; Richard, P.; Poli, R. *Inorg. Chem.* **2001**, *40*, 1597. (c) Anderson, J. C.; Cubbon, R. J.; Harling, J. D. *Tetrahedron: Asymmetry* **1999**, *10*, 2829. (d) Anderson, J. C.; Cubbon, R. J.; Harling, J. D. *Tetrahedron: Asymmetry* **2001**, *12*, 923. (e) Dahlenburg, L.; Götz, R. J. *Organomet. Chem.* **2001**, *619*, 88. (f) Berger, H.; Nesper, R.; Pregosin, P. S.; Rüegger, H.; Wörle, M. *HCA* **1993**, *76*, 1520. (g) Hayashi, T.; Konishi, M.; Fukushima, M.; Kanehira, K.; Hioki, T.; Kumada, M. *J. Org. Chem.* **1983**, *48*, 2195. (h) Kinoshita, I.; Kashiwabara, K.; Fujita, J. *Chem. Lett.* **1977**, 831. (i) Nagel, U.; Nedden, H. G. *Chem. Ber.* **1997**, *130*, 989. (j) Bianchini, C.; Cicchi, S.; Peruzzini, M.; Pietrusiewicz, K. M.; Brandi, A. *J. Chem. Soc., Chem. Commun.* **1995**, 833. (k) Mino, T.; Wakui, K.; Oishi, S.; Hattori, Y.; Sakamoto, M.; Fujita, T. *Tetrahedron: Asymmetry* **2008**, *19*, 2711.
- 6 (a) Chen, G. S.; Li, X.; Zhang, H. L.; Gong, L. Z.; Mi, A. Q.; Cui, X.; Jiang, Y. Z.; Choi, M. C. K.; Chan, A. S. C. *Tetrahedron: Asymmetry* **2002**, *13*, 809. (b) Vasconcelos, I. C. F.; Rath, N. P.; Spilling, C. D. *Tetrahedron: Asymmetry* **1998**, *9*, 937.
- 7 Schnitzler, V.; Nonglaton, G.; Roussière, H.; Maillet, C.; Evain, M.; Janvier, P.; Bujoli, B.; Petit, M. *Organometallics* **2008**, *27*, 5997.
- 8 Carroll, M. P.; Guiry, P. J.; Brown, J. M. *Org. Biomol. Chem.* **2013**, *11*, 4591.
- 9 Habtemariam, A.; Watchman, B.; Potter, B. S.; Palmer, R.; Parsons, S.; Parkin, A.; Sadler, P. J. *J. Chem. Soc. Dalton Trans.* **2001**, 1306.
- 10 (a) Farkas, G.; Császár Zs.; Balogh, Sz.; Tóth, I.; Bakos, J. *Tetrahedron Letters* **2014**, *55*, 4120. (b) Balogh, Sz.; Farkas, G.; Madarász, J.; Szöllősy, Á.; Kovács, J.; Darvas, F.; Ürge, L.; Bakos, J. *Green Chem.* **2012**, *14*, 1146.
- 11 Eliel, E. L.; Wilen, S. H. (1994) Stereochemistry of Organic Compounds, John Wiley, Chichester.
- 12 Cremer, D.; Pople, J. A. *J. Am. Chem. Soc.* **1975**, *97*, 1354.
- 13 Bentruude, W. G.; Setzer, W. N. „Stereospecificity in 31P-Element Couplings: Proton-Phosphorus Couplings“ in Phosphorus-31 NMR Spectroscopy in Stereochemical Analysis (eds. Verkade, J. G. and Quin, L. D.), 1987 VCH Publishers, Inc., Deerfield Beach, Florida pages 365-389 and referencies therein.
- 14 Structure Determination Using NMR, Online NMR course Hans J. Reich, University of Wisconsin, 2013 and references therein.
- 15 (a) Kollmar, M.; Steinhagen, H.; Janssen, G. P.; Goldfuss, B.; Malinovskaya, S. A.; Vazquez, J.; Rominger, F.; Helmchen, G. *Chem. Eur. J.* **2002**, *8*, 3103. (b) Helmchen, G. *J. Organomet. Chem.* **1999**, *576*, 203. (c) Armstrong, P. B.; Dembicser, E. A.; Desbois, A. J.; Fitzgerald, J. T.; Gehrmann, J. K.; Nelson, N. C.; Noble, A.L.; Bunt, R. C. *Organometallics*, **2012**, *31*, 6933. (d) Zehnder, M.; Schaffner, S.; Neuburger, M.; Plattner, D. A. *Inorg. Chim. Acta*, **2002**, *337*, 287.
- 16 (a) McManus, H. A.; Guiry, P. J. *Chem. Rev.* **2004**, *104*, 4151. (b) McManus, H. A.; Cusack, D.; Guiry, P. J. P/Oxazoline Ligands. In: Phosphorus Ligands in Asymmetric Catalysis; Börner, A., Ed.; Wiley-VCH, Verlag GmbH & Co. KGaA: Weinheim, **2008**, Vol. 2, pp. 549-595. (c) von Matt, P.; Pfalz, A. *Angew. Chem. Int. Ed. Engl.* **1993**, *32*, 566.
- 17 (a) Helmchen, G.; Pfaltz, A. *Acc. Chem. Res.* **2000**, *33*, 336. (b) Helmchen, G.; Wiese, B.; *Tetrahedron Lett.* **1998**, *39*, 5727. (c) Helmchen, G. *J. Organomet. Chem.* **1999**, *576*, 203.
- 18 According to the ¹³C NMR spectrum of complex **3a**, the carbon *trans* to the P is more electrophilic than that *trans* to N. X-ray structures and DFT geometry optimizations proved that Cl-Pd or C-Pd bonds are longer *trans* to the P compared to that *trans* to N.

- These observations confirm the hypothesis that the bond *trans*-to-P is the more susceptible to be cleaved by the nucleophile.
- 19 (a) Helmchen, G.; Kudis, S.; Sennhenn, P.; Steinhagen, H. *Pure Appl. Chem.* **1997**, *69*, 513. (b) Anderson, J. C.; James, S. D.; Mathias, J. P. *Tetrahedron: Asymmetry* **1998**, *9*, 753. (c) von Matt, P.; Loiseleur, O.; Koch, G.; Pfaltz, A.; Lefeber, C.; Fuecht, T.; Helmchen, G. *Tetrahedron: Asymmetry* **1994**, *5*, 537. (d) Brown, J. M.; Hulmes, D. I.; Guiry, P. J. *Tetrahedron* **1994**, *50*, 4493. (e) Burckhardt, U.; Hintermann, L.; Schnyder, A.; Togni, A. *Organometallics*, **1995**, *14*, 5415.
- 20 Porte, A.; Reibenspies, J.; Burgess, K. *J. Am. Chem. Soc.* **1998**, *120*, 9180.
- 21 Drew, D.; Doyle, J. R. *Inorg. Synth.* **1972**, *13*, 52.
- 22 von Matt, P.; Lloyd-Jones, G. C.; Minidis, A. B. E.; Pfaltz, A.; Macko, L.; Neuburger, M.; Zehnder, M.; Rüegger, H.; Pregosin, P. *S. Helv. Chim. Acta* **1995**, *78*, 265.